isotopic substitution are the equilibria among the boat-chair conformers of unsymmetrically deuterated cyclooctanone-2-D. Any particular hydrogen at C-2, C-3 or C-4 exchanges among four possible environments ($\alpha$ or $\alpha'$, $\beta$ or $\beta'$, or $\gamma$ or $\gamma'$, and axial or equatorial). If a single deuterium is substituted for a hydrogen at C-2, the four conformers are diastereomeric and equilibrium isotope effects may occur in which each comformer contributes a different amount to the equilibrium. However, since only two carbon environments can be distinguished, the apparent equilibrium will be between two pairs of conformers, *i.e.*, [1B + 1C]$\rightleftarrows$[1A + 1D] as shown in Figure 2. The equilibrium isotope shifts in $^{13}C$ spectra can be used to detect the proportion of time C-2 is in each environment, $\alpha$ and $\alpha'$, but cannot reveal the position of 1B$\rightleftarrows$1C or 1A$\rightleftarrows$1D equilibria. The situation is simpler if both hydrogens at a carbon are substituted by deuterium, because then the 1B$\rightleftarrows$1C equilibrium is degenerate, the 1A$\rightleftarrows$1D equilibrium is degenerate and the observed equilibrium is between only two different conformers.

When equilibrium constants were derived from equilibrium isotope shifts using Saunder's equation, the equilibrium constants were always expressed as values greater than unity, $K > 1$. The direction of the isotope effect can be determined by noting whether individual carbons move toward upfield or downfield by the equilibrium isotope shift. It was shown that $\alpha$, $\beta'$, and $\gamma$ carbons appear upfield of the corresponding $\alpha'$, $\beta$, and $\gamma'$ carbons. If C-2 is moved upfield and C-8 downfield by the isotope effect, it is clear that C-2 resides more of time in the $\alpha$ environment, C-8 is correspondingly more in the $\alpha'$ environment. The average environment for C-2 and C-8 would differ, with C-2 shifted upfield of the reference peak and C-8 shifted downfield by an equal amount. Deuterium labeling at C-2 position in a cyclooctanone causes the intrinsic and equilibrium isotope effects by causing deviations in the relative populations of B+C and A+D involved in the equilibrium.

## References

1. (a) Hansen, P. E. *Ann. Rept. NMR Spectr* **1983**, *15*, 105. (b) Forsyth, D. A.; Buncel, E.; Lee, Elsevier C. C., Ed.; Isotopes in Organic Chemistry: New York, 1984; Vol. 6, Chap. 1. (c) Nakashima, Y.; Sone, T.; Teranishi, D.; Suzuki, T. K.; Takahash, K. *Magn. Reson. in Chem.* **1994**, *32*, 578.
2. Berger, S.; Diehl, B. W. K.; Kunzer, H. *Chem. Ber.* **1987**, *120*, 1059.
3. Saunders, M.; Jaffe, M.; Vogel, P. *J. Am. Chem. Soc.* **1971**, *93*, 2558
4. Jung, M. W. *Bull. Korean Chem. Soc.* **1991**, *12*, 224.
5. Jung, M. W. *Anal. Sci. and Tech.* **1994**, *7*(2), 213.
6. Nakashima, Y.; Kanada, H.; Fukunaga, M.; Suzuki, K.; Takahashi, K. *Bull. Chem. Soc. Jpn.* **1992**, *65*, 2894.
7. Butiz-Hermandez, H.; Bernheim, R. A. *Prog, Nucl. Magn. Reson. Spectr.* **1967**, *3*, 63.

# Studies of the Pyrrhotite Depression Mechanism with Diethylenetriamine

**Dong-Su Kim**

*Department of Environmental Sci. and Eng., Ewha Womans University, Seoul 120-750, Korea*
*Received February 18, 1998*

The mechanism by which pyrrhotite is depressed by diethylenetriamine (DETA) during pentlandite flotation has been studied. Amyl xanthate is observed to adsorb on pyrrhotite to form both dixanthogen and iron xanthate. In the presence of DETA, the amount of xanthate adsorbed on pyrrhotite is substantially reduced as evidenced by infrared and UV/Vis spectroscopy. However, DETA does not adsorb on pyrrhotite as evidenced by infrared and X-ray photoelectron spectroscopy. DETA shifts the potential of the onset of xanthate adsorption on pyrrhotite by approximately 200 mV toward anodic direction, which is thought to be due to the increased solubility of surface oxidized species on pyrrhotite in the presence of DETA. A window of selectivity for the separation of pentlandite and pyrrhotite is provided by the results obtained in this study.

## Introduction

Recently, diethylenetriamine (DETA) has been used as a depressant for pyrrhotite in the mining industry. DETA makes it possible to remove pyrrhotite more efficiently, while increasing the recovery of copper, nickel, and platinum. Plant experience shows that DETA is most effective at pH 9-9.5, works best under highly oxidizing conditions, and is sensitive to water chemistry.

Although the effectiveness of DETA as a pyrrhotite depressant has been verified in plant practice, its mechanism is not well understood. everal different mechanisms may be speculated based on the general chemistry of DETA and the operating experience at the mill:

1. DETA could adsorb on pyrrhotite selectively to passivate the mineral, thereby preventing xanthate adsorption.

2. Iron hydroxy-DETA complexes may adsorb on pyrrhotite selectively, rendering the surface hydrophilic.

3. DETA-dixanthogen complexes may adsorb on the surface with an orientation that renders the surface hydrophilic.

4. DETA may control the electrochemical potential of the system by complexing $Fe^{3+}$ (or $Fe^{2+}$) ions.

5. DETA may control the pulp potential by forming complexes with transition metal ions that can bind molecular oxygen.

The first three possible mechanisms involve adsorption of DETA on pyrrhotite, while the last two suggest indirect mechanisms. It was suggested that DETA may reduce the potential below that of the xanthate/dixanthogen couple, preventing xanthate adsorption on pyrrhotite.[1]

In this study, the adsorption characteristics of DETA on pyrrhotite was examined by mainly spectroscopic measurements, which is related to the first three possibilities. The spectroscopic work included Fourier Transform Infrared (FTIR), X-ray photoelectron spectroscopy (XPS), and UV/Vis spectroscopic analyses.

Understanding how DETA depresses pyrrhotite should not only help industry optimize the performance of this particular reagent, but should also help them find more powerful depressants in the future. Since DETA is very different from other flotation reagents commonly used in industry today, the improved understanding of the reaction mechanism(s) may eventually lead industry to develop new breeds of flotation reagents.

## Experimental

**Materials.** Natural pyrrhotite specimens received from INCO (Canada) were cut by a diamond saw to 15 40 mm plates, rough-polished using 600 grit silicon carbide paper and fine-polished using 0.3 and 0.05 m alumina powders. After polishing, the electrodes were washed in an ultrasonic bath in warm ethyl alcohol, and then in 18 MΩ deionized water. A reagent grade DETA (99% purity) was obtained from Aldrich Chemicals. The potassium amyl xanthate (KAX) was recrystallized three times with acetone and ethyl ether before use. KAX was oxidized to its dimer, diamyl dixanthogen ($(AX)_2$), using iodine solution to obtain the standard FTIR spectrum.

All measurements were conducted at pH 9.2 in 0.05 M $Na_2B_4O_7$ buffer solution. The borate was of analytical grade and the solutions were prepared using 18 MΩ deionized water. Prior to each measurement, the solution was deoxygenated by purging with low-oxygen (< 0.05 ppm $O_2$) nitrogen gas for at least one hour.

**FTIR Spectroscopy Measurements.** FTIR spectroscopic measurements were conducted on pyrrhotite electrodes under open-circuit and controlled-potential conditions at pH 9.2 using an external reflection attachment (Spectra Tech) with a single reflection. The spectra were recorded using a Bio-Rad FTS 60A FTIR spectrometer with a liquid nitrogen-cooled MCT detector. A total of 64 scans were recorded at 4 $cm^{-1}$ resolution, co-added, and signal-averaged for each measurement. A wire grid polarizer was used to polarize the incident beam.

**XPS Measurements.** The XPS measurements were carried out using a Kratos XSAM 800 spectrometer at a vacuum pressure of approximately $10^{-7}$ Pa. Unmonochromatized X-rays from a magnesium anode (operated at 13 kV and 18 mA) were used to excite the photoelectrons. A slit width of 2 mm was used for measuring the individual lines to get an optimal resolution. Under these conditions, the full width at half maximum (FWHM) of the Ag (3d3/2) peak was 1.1 eV. The energy scale was calibrated by using the Au (4f7/2) line (Binding Energy, BE 84.0 eV) and the Cu (2p3/2) line (BE 932.6 eV). Binding energy shifts due to charging were corrected by using the C (1s) line (BE 285.0 eV).

**UV/Vis Spectroscopy Measurements.** The solution was analyzed for DETA and KAX using a Perkin-Elmer Lambda Array 3840 UV/Vis Spectrophotometer. A 1-cm pathlength quartz cell was used for the measurements. The absorbance of the DETA and KAX solutions were measured at 206 and 303 nm, respectively.

After contacting a pulverized pyrrhotite sample (20×30 mesh) for ten minutes with the DETA and/or KAX solutions, the clear solution was recovered by passing it through a 0.2 μm filter. The solution was then transferred to a quartz cell to take the spectra. It should be noted that the 206 line for DETA was too close to that for oxygen and that the oxidation products derived from pyrrhotite changed the baseline significantly, making measurement difficult.

**Contact Angle Measurements.** A specially-designed electrochemical cell was used to measure contact angles under controlled potential conditions.[2] The pyrrhotite electrode was polarized at a cathodic potential to remove any oxidation products from the surface. The potential was then increased to a desired value before bringing a nitrogen bubble to the electrode surface to make the contact. The electrode was held in an upright position, and the equilibrium contact angles were measured using a Rame-Hart Model 100 Goniometer.

**Voltammetry.** The voltammetry experiments were conducted using a conventional three-electrode circuit. The electrode potential was controlled with a PAR Model 371 Potentiostat/Galvanostat and a PAR Model 175 Universal Programmer. Although an Ag/AgCl electrode was used as the reference electrode, the potentials reported here are expressed on the standard hydrogen electrode (SHE) scale.

## Result and Discussion

**FTIR Spectroscopic Stdies.** The spectra of KAX, $(AX)_2$, and DETA are given in Figure 1. In the "fingerprint region" (950 1350 $cm^{-1}$), KAX gives a strong band at 1074 $cm^{-1}$ due to the C=S stretching vibration and at 1137 $cm^{-1}$ due to the symmetric C=O=C vibrations.[3] The minor band at 1249 $cm^{-1}$ is attributed to a combination of S-C-S and C-O-C asymmetric vibrations. The $(AX)_2$ spectrum shows the characteristic peak at 1259 $cm^{-1}$ with a shoulder at 1207 $cm^{-1}$, which are due to S-C-S and C-O-C vibrations.[4] The two strong bands at 1043 and 1023 $cm^{-1}$ are due to C=S stretching vibrations. The small peak at 1123 $cm^{-1}$ is attributed to C-O-C stretching vibrations.

The DETA spectrum shows a major absorption band at 1574 $cm^{-1}$ due to N-H vibrations and two other bands at 1487 and 1120 $cm^{-1}$ due to C-N vibrations.[5] The bands at 1436, 1317 and 819 $cm^{-1}$ are probably due to the $CH_2$ group vibrations.

Figure 2 shows the FTIR spectrum (bottom of Figure 2) of the pyrrhotite electrode conditioned in a $10^{-3}$ M KAX

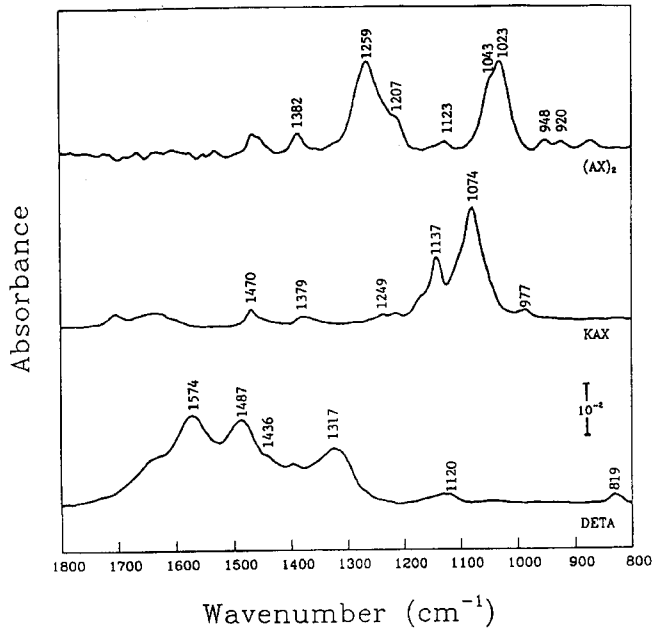


**Figure 1.** FTIR spectra of DETA, KAX and $(AX)_2$.

solution for ten minutes at open-circuit. The presence of dixanthogen on the pyrrhotite surface was indicated by the peaks at 1259, 1207 and 1043 $cm^{-1}$. There are also indications of iron xanthate co-existing with dixanthogen on the mineral surface, as evidenced by i) the increase in the 1207 $cm^{-1}$ band (relative to the 1259 $cm^{-1}$ band), and ii) broadening and shifting of the C-O-C (1123 $cm^{-1}$) and C=S vibrations (1023 $cm^{-1}$) to 1136 and 1016 $cm^{-1}$, respectively. The FTIR external reflection spectroscopic studies conducted by other investigators also showed the co-adsorption of iron xanthate and dixanthogen for the ethyl xanthate-marcasite[6] and amyl xanthate-pyrite[7] systems. However, an *in-situ* FTIR study showed that only diethyl dixanthogen is formed on pyrrhotite at open-circuit conditions.[8] Since the external reflection measurement employed in the present work is an *ex-situ* technique, the difference like this is considered to be observed.

After taking the spectrum, the pyrrhotite electrode that had been contacted with a $10^{-3}$ M KAX solution was conditioned in a $10^{-3}$ M DETA solution for ten minutes. As shown in Figure 2 (top spectrum), the intensity of the characteristic dixanthogen bands decreased, while that of iron xanthate did not, suggesting that dixanthogen may be displaced by DETA from the pyrrhotite surface. However, the spectrum does not show the presence of DETA on the surface, minimizing the possibility of DETA displacing dixanthogen from the surface. There is another possible explanation for the decrease in the amount of dixanthogen on pyrrhotite surface, *i.e.*, evaporation. Amyl dixanthogen has considerable vapor pressure, and the long exposure time associated with the *ex-situ* FTIR measurement after the DETA treatment may be sufficient to lose some dixanthogen; however, the following set of experiments seemed to dispel the possibility of dixanthogen evaporation.

Figure 3 (top) showed no indications of DETA adsorption on a pyrrhotite sample contacted with $10^{-3}$ M DETA solution at open circuit. Using a reverse sequence of conditioning (*i.e.* DETA treatment followed by contacting with a $10^{-3}$ M KAX solution), there was an indication of xanthate adsorption (Figure 3, middle) as evidenced by the broad band at around 1055 $cm^{-1}$; however, the signal intensities of the adsorbed xanthate were substantially lower than that without DETA (Figure 2, bottom). The spectrum

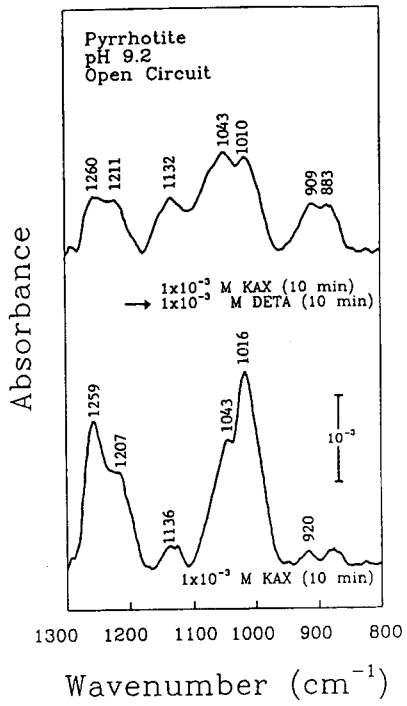


**Figure 2.** FTIR spectra of pyrrhotite conditioned at pH 9.2 in $10^{-3}$ M KAX solution for 10 min initially (bottom) and then in $10^{-3}$ M DETA solution (top).

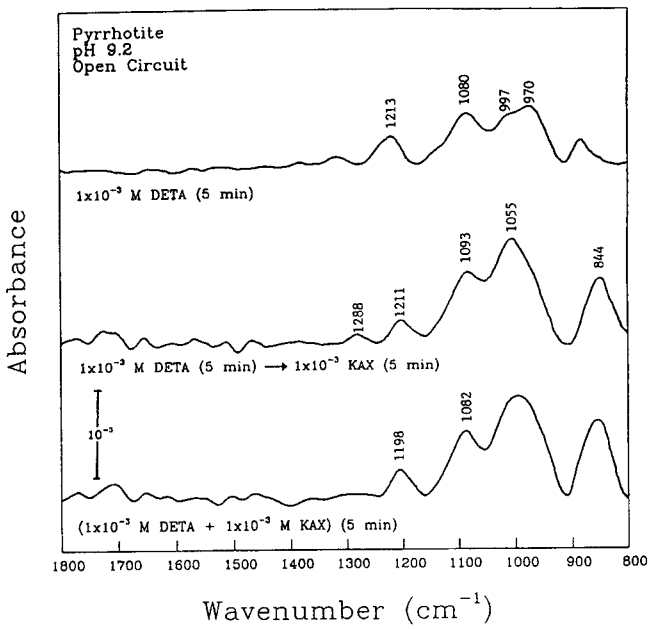


**Figure 3.** FTIR spectra of pyrrhotite conditioned at pH 9.2 in $10^{-3}$ M DETA solution initially (top), and then in $10^{-3}$ M KAX solution (middle). Also shown is the FTIR spectra of pyrrhotite conditioned in a solution containing both $10^{-3}$ M KAX and $10^{-3}$ M DETA (bottom).

obtained after conditioning in a solution containing both KAX ($10^{-3}$ M) and DETA ($10^{-3}$ M) also showed a very small amount of xanthate adsorbed on the mineral surface (Figure 3, bottom). It is interesting to note that the adsorbed xanthate species in both experiments were mostly iron xanthates (Figure 3, middle and bottom). Evidently, DETA inhibits xanthate adsorption, particularly dixanthogen, on pyrrhotite regardless of the sequence of reagent addition.

Figure 4 shows the FTIR spectra obtained after conditioning the pyrrhotite sample for five minutes in $10^{-3}$ M KAX solutions at pH 9.2 under controlled-potential conditions. The sample was removed from the cell, rinsed with deionized water, dried by blowing the surface with nitrogen, then placed in the spectrometer to take the external reflectance spectrum. There are no indications of xanthate adsorption at $-0.3$ V. Although not shown here, the xanthate adsorption begins at approximately 0 V. The spectrum obtained at 0.2 V shows absorption bands characteristic of adsorbed dixanthogen at 1260, 1136, 1048 and 1015 $cm^{-1}$. The appearance of the 1227 $cm^{-1}$ band indicates iron xanthate formation. Note that the intensity ratio between the 1224-1227 and the 1256-1262 $cm^{-1}$ bands increases with increasing potential, suggesting that iron xanthate formation becomes more favored at high potentials where the activity of iron hydroxide is high due to anodic oxidation. At 0.4 V, pyrrhotite itself was severely oxidized as indicated by a broad band in the 980-1150 $cm^{-1}$ region.

The FTIR results given in Figure 4 seem to support the xanthate adsorption mechanism proposed by Hodgson and Agar.[9] Based on voltammetry studies, they suggest that pyrrhotite oxidizes as follows:

$$FeS + H_2O = Fe(OH)[S]^+ + H^+ + 2e \quad (1)$$

to form an iron (III) hydroxy-polysulfide as the initial oxidation product. Xanthate ions adsorb on the positively-charged oxidation product *via* coulombic attraction:

$$Fe(OH)[S]^+ + X^- = Fe(OH)[S]X, \quad (2)$$

to form an iron (III) hydroxy-polysulfide xanthate on the surface, while the residual xanthate is subsequently oxidized to dixanthogen.

Figure 5 shows the FTIR spectra of pyrrhotite conditioned in $10^{-3}$ M DETA solution at different potentials. There are no indications of DETA adsorption over the entire potential region studied. Only the oxidation products of the mineral, as indicated by the bands in the 900 1200 $cm^{-1}$ region, were observed. Note that the spectra shown in Figure 5 were obtained by subtracting the spectrum of unoxidized pyrrhotite and water adsorbed on pyrrhotite, so that the IR bands due to adsorbed DETA can be seen more clearly. Unfortunately, the characteristic IR bands for DETA are in the range of those for adsorbed water molecules; therefore, the sensitivity for detecting DETA on the surface of pyrrhotite depends on the amounts of water present on the pyrrhotite surfaces. Although the spectra given in Figure 5 show no evidence for DETA adsorption, further studies may be required to substantiate the evidence that DETA does not adsorb on pyrrhotite.

Figure 6 shows the spectra of pyrrhotite conditioned in a solution containing $10^{-3}$ M KAX and DETA at various potentials. In the presence of DETA, xanthate adsorption is significantly reduced. There are indications of xanthate adsorption at higher potentials, but the amount adsorbed is very small when compared with those without DETA (Figure 4).

To see the effect of DETA on xanthate adsorption more closely, the spectra obtained in $10^{-3}$ M KAX solutions with and without $10^{-3}$ M DETA at 0.3 V are compared in Figure 7. In the presence of DETA, the amount of adsorbed xanthate was reduced drastically, demonstrating the ef-

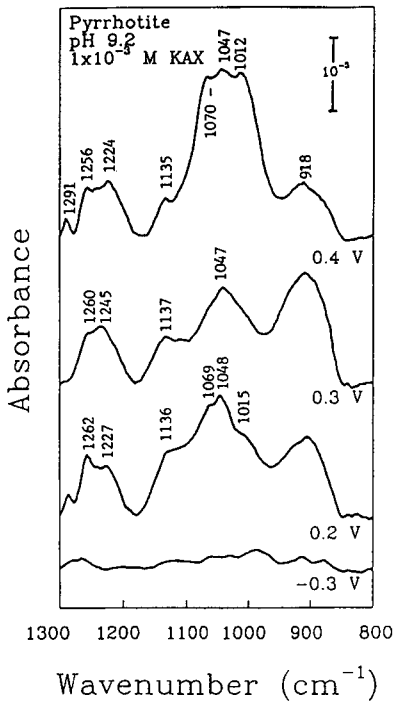


**Figure 4.** FTIR spectra of pyrrhotite at pH 9.2 conditioned in $10^{-3}$ M KAX solution at different potential conditions.

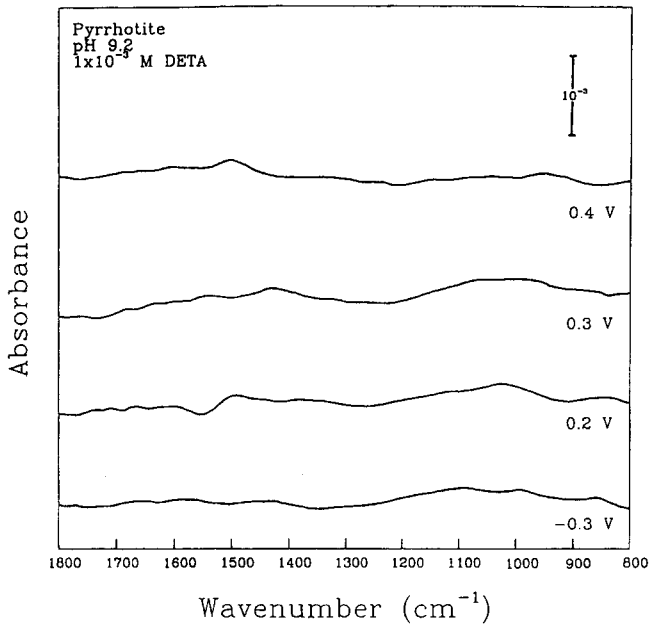


**Figure 5.** FTIR spectra of pyrrhotite at pH 9.2 conditioned in $10^{-3}$ M DETA solution at different potential conditions.

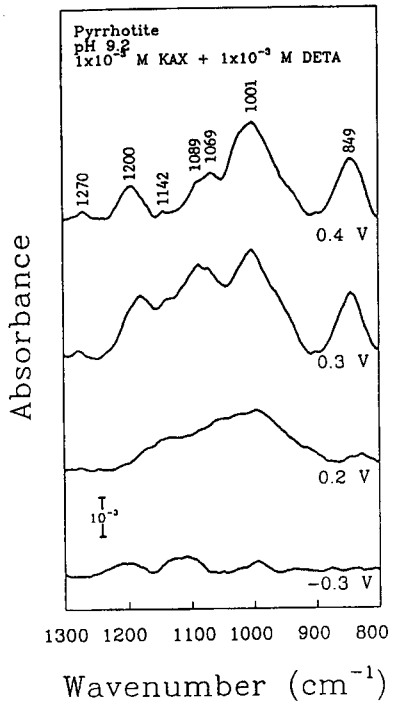


**Figure 6.** FTIR spectra of pyrrhotite at pH 9.2 conditioned in a mixture of $10^{-3}$ M KAX and $10^{-3}$ M DETA solution at different potential conditions.

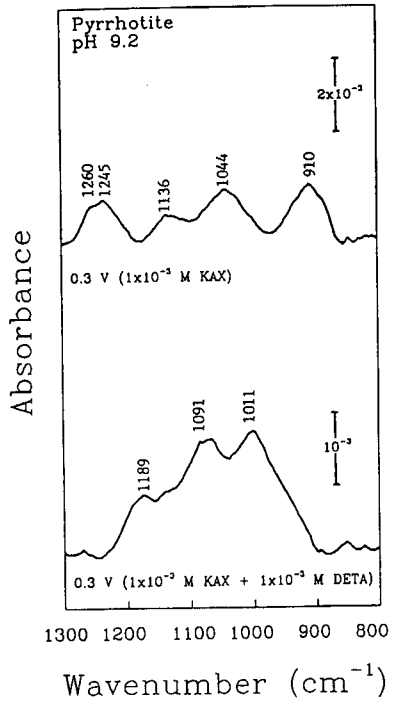


**Figure 7.** FTIR spectra of pyrrhotite at pH 9.2 conditioned in a mixture of $10^{-3}$ M KAX and $10^{-3}$ M DETA solution at 0.3 V.

fectiveness of DETA as a pyrrhotite depressant. It is also interesting to see that in the presence of DETA the mineral becomes more severely oxidized as indicated by the strong bands in the 980-1200 $cm^{-1}$ region. This finding is substantiated by the voltammetry results which will be discussed later.

In Figure 8, the IR signal intensities, as measured at 1256-1262 $cm^{-1}$, and the contact angle data are plotted as a function of applied potential. No discernable hydrophobicity is observed in the buffer solution or in $10^{-3}$ M DETA solution without xanthate. In $10^{-3}$ M KAX solution, the pyrrhotite electrode becomes hydrophobic above 0 V, which is close to the reversible potential of the following reaction:

$$2X^- = X_2 + 2e \quad (3)$$

whose $E_r$ is 0.047 V at [KAX]=$10^{-3}$ M. The FTIR data show the same trend. In the presence of both DETA and KAX, the potential where xanthate begins to adsorb on pyrrhotite (as indicated by the changes in IR intensities) and where the mineral becomes hydrophobic shifts by about 0.2 V.

One possible explanation for this shift in the potential is that DETA may complex with the $Fe^{3+}$ ions (or with its hydroxy complexes) in solution, resulting in a decrease in the activity of free ions in solution. This in turn increases the solubility of the iron hydroxy-polysulfide and, hence, decreases its surface activity. Increased solubility of the pyrrhotite oxidation product will be shown by the voltammetry results. According to the Nernst equation, a decrease in the surface activity of the iron hydroxy-polysulfide will shift the reversible potential of reaction (1) towards an anodic direction. If reaction (1) is the precursor for xanthate adsorption (reaction (2)), the onset of xanthate adsorption should, therefore, occur at higher potentials.

**XPS Studies.** To determine whether DETA adsorbs on pyrrhotite, the XPS spectra of the mineral were taken after conditioning the mineral for 5 minutes in the pH 9.2 buffer solution containing $10^{-4}$ M DETA at open circuit conditions. The results given in Table 1 showed no changes in either the binding energy or the amount of nitrogen present on the pyrrhotite surface before and after the DETA treatment; however, the intensity of the carbon peak increased considerably. Knowing that carbon contamination is quite common during XPS measurements, the data obtained may suggest that DETA does not adsorb on pyrrhotite.

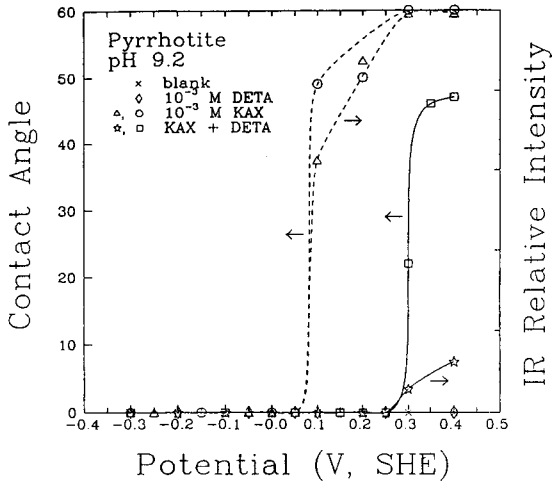


**Figure 8.** Effect of potential on the contact angle and IR relative intensity measured for pyrrhotite at pH 9.2 in buffer solution (x), $10^{-3}$ M DETA solution (◇), $10^{-3}$ M KAX (○, △) and a mixture of $10^{-3}$ M KAX and $10^{-3}$ M DETA solution (□, ★).

**Table 1.** XPS results for pyrrhotite conditioned in 0 and $10^{-4}$ M DETA solutions

| [DETA] | S2p | | Fe3p | | N1s | | O1s | | C1s | |
|---|---|---|---|---|---|---|---|---|---|---|
| | B.E.[a] | At.%[b] | B.E. | At.% | B.E. | At.% | B.E. | At.% | B.E. | At.% |
| 0 | 160.7 | 15.0 | 54.0 | 11.0 | 400.0 | 2.0 | 532.0 | 33.0 | 285.0 | 39.0 |
| $10^{-4}$ | 160.6 | 14.4 | 54.0 | 10.6 | 399.9 | 2.1 | 532.1 | 25.7 | 285.0 | 47.0 |

[a] Binding energy. [b] Calculated atomic percentage.

**UV/Vis Spectroscopy Studies.** The adsorption of DETA on pyrrhotite was investigated by monitoring the DETA concentration in solution using the UV/Vis spectroscopy. There were no changes in the amount of DETA present in solution before and after contacting the $10^{-5}$ M DETA solution with pyrrhotite for ten minutes. This indicates that DETA does not adsorb on pyrrhotite, which agrees with the FTIR and XPS spectroscopic data.

The effect of DETA on KAX adsorption on pyrrhotite was also studied by monitoring the xanthate concentration in solution. Figure 9 shows the xanthate spectra obtained under various conditions. All measurements were conducted in a 0.05 M borate buffer (pH 9.2) solution. After ten minutes of contact time at open circuit, the xanthate concentration was reduced by 40% (as measured by the UV absorbance at 303 nm), indicating significant adsorption. In the presence of $10^{-5}$ M DETA, the xanthate concentration was reduced by only 10%. This finding further substantiates the conclusion from FTIR and contact angle work that DETA inhibits xanthate adsorption on pyrrhotite.

**Voltammetry.** Figure 10 shows the voltammograms of pyrrhotite obtained in the absence and presence of $10^{-3}$ M KAX at 50 mV/sec. In the absence of xanthate and stirring, the anodic oxidation current was observed starting at about 0 V. When the solution was stirred, the anodic current was higher and started at approximately −300 mV. A similar observation was made by other investigators,[10] who attributed the increase in anodic current to the initial oxidation product (*i.e.* Fe(OH)[S] ) being soluble as suggested by reaction (1). At higher potentials, however, insoluble (and thermodynamically more stable) oxidation products such as $Fe(OH)_3$ and $S^0$ would be formed. In this case, the voltammograms obtained during the cathodic scan with and without stirring should be indistinguishable from each other, as shown in Figure 10 and reported in previous work.[10,11] In the presence of $10^{-3}$ M KAX, the anodic current was reduced considerably at low potentials, indicating that the xanthate adsorption passivated pyrrhotite oxidation. There were no new peaks attributable to xanthate adsorption or oxidation.

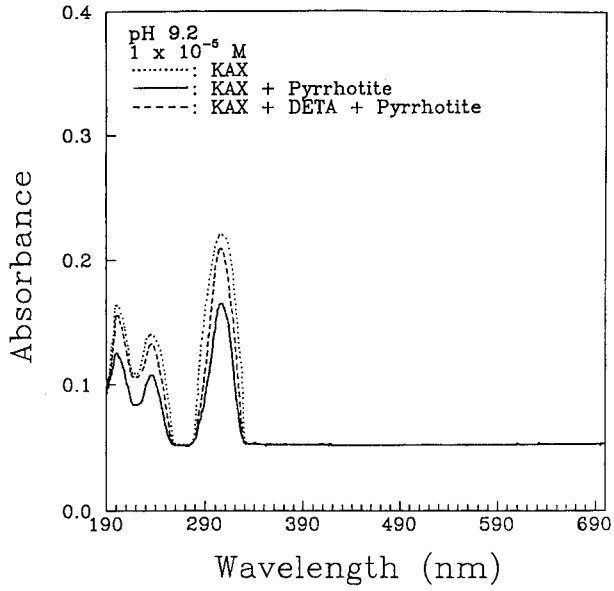


**Figure 9.** UV/Vis spectra recorded for a pH 9.2 solution a) initially containing $10^{-5}$ M KAX, b) after pyrrhotite conditioning for 10 minutes, and c) KAX and $10^{-5}$ M DETA after pyrrhotite conditioning.

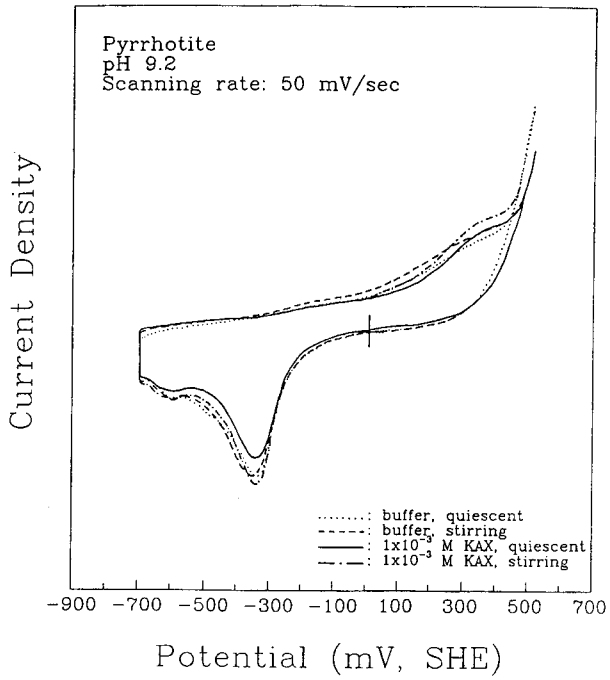


**Figure 10.** Voltammograms for pyrrhotite at pH 9.2 in 0 and $10^{-3}$ M KAX solution.

Figure 11 shows the voltammograms of pyrrhotite obtained in the absence and presence of $10^{-3}$ M DETA. In the presence of DETA, the anodic currents increased, becoming more significant when the solution was stirred. These findings indicate that the oxidation product (*e.g.*, Fe(OH)[S] formed as a result of reaction (1)) has considerable solubility in the 0.05 M borate buffer solution. As shown in Figure 11, the solubility increased in the presence of DETA. According to Rao and Finch,[12] only the iron hydroxide dissolves into solution, leaving the polysulfide behind on the surface. The latter may be further oxidized to longer chain polysulfides or elemental sulfur, both of which are insoluble species.

Figure 11 also shows that in the presence of DETA, a new cathodic reduction peak was observed near −420 mV, possibly indicating the reduction of the longer chain polysulfides or elemental sulfur formed after losing part of the iron hydroxide into solution. Therefore, it is clear that the role of DETA is to modify the redox behavior of pyrrhotite.

Figure 12 shows the voltammograms of pyrrhotite ob-

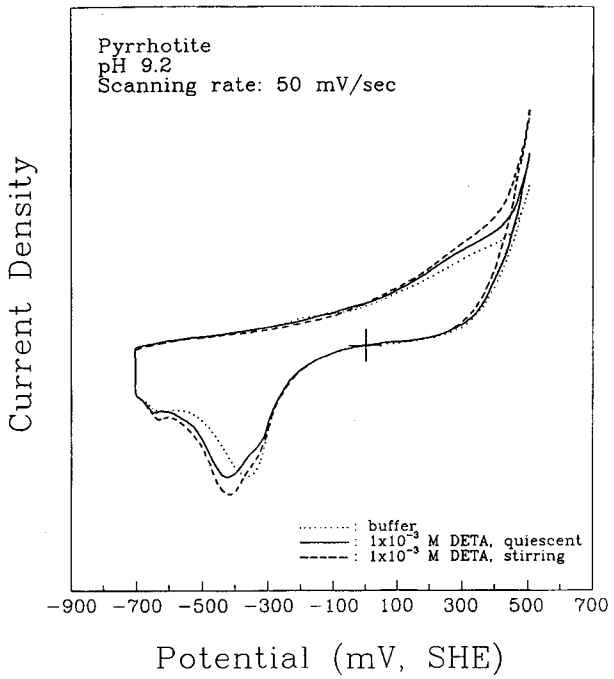


**Figure 11.** Voltammograms for pyrrhotite at pH 9.2 in 0 and $10^{-3}$ M DETA solution.

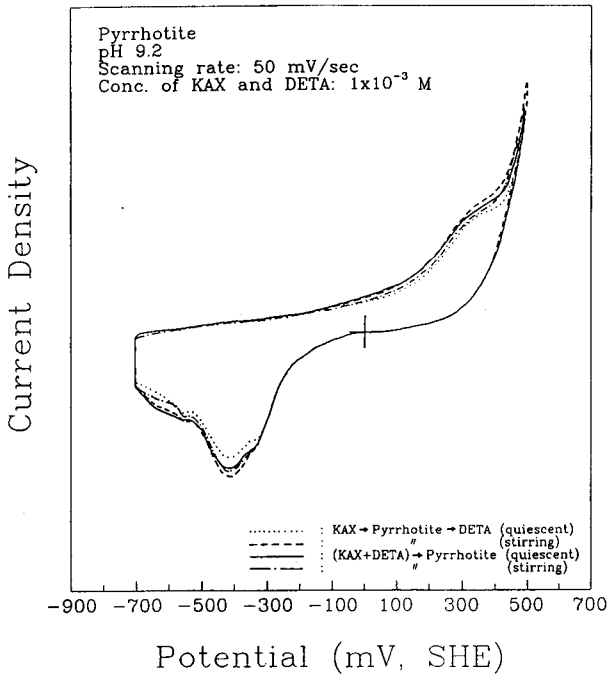


**Figure 12.** Voltammograms for pyrrhotite at pH 9.2 in 0 and $10^{-3}$ M KAX+$10^{-3}$ M DETA solution.

tained in the presence of both DETA and KAX ($10^{-3}$ M). At potentials below approximately 200 mV, the anodic currents were smaller than with DETA alone. At higher potentials, however, the anodic current increased in the presence of xanthate. It should also be noted that the cathodic waves were considerably different from those obtained with DETA alone. The height of the largest cathodic peak observed in the presence of DETA was slightly reduced and new cathodic peaks were observed in the presence of KAX near − 550 mV. This result also substantiates that the electrochemical behavior of pyrrhotite depends much on the existence of DETA in the solution.

## Conclusions

1. The FTIR spectroscopic studies show that amyl xanthate adsorbs on pyrrhotite to form both dixanthogen and iron xanthate. This finding substantiates the mechanism that part of the xanthate reacts with iron hydroxy-polysulfide (produced as a result of pyrrhotite oxidation) to form iron xanthate and the rest is oxidized to form dixanthogen.

2. The FTIR spectroscopic studies show that the amount of xanthate adsorbed on pyrrhotite decreases substantially in the presence of DETA. However, there are no indications of DETA adsorbing on pyrrhotite in place of xanthate, which is also supported by the results obtained from XPS and UV/Vis spectroscopic analysis.

3. The contact angle and FTIR spectroscopy studies conducted under controlled potential conditions show that in the presence of DETA the potential at which xanthate begins to adsorb on pyrrhotite shifts by approximately 200 mV to anodic direction. This potential shift for the onset of collector adsorption may provide an explanation for the window of selectivity between pentlandite and pyrrhotite.

4. The anodic potential shift for the onset of xanthate adsorption may be explained by the increased solubility of the iron hydroxy-polysulfide formed as a result of pyrrhotite oxidation. Evidence for the increased solubility of the pyrrhotite oxidation product is given by voltammetry and FTIR results.

## References

1. Leppinen, J. O.; Basilio, C. I.; Yoon, R. H. *Int. J. Miner. Process.* **1989**, *26*, 259.
2. Basilio, C. I. *Ph.D. Thesis*, Virginia Polytechnic Institute and State University, Blacksburg, VA, 1989.
3. Little, L. H.; Poling, G. W.; Leja, J. *Can. J. Chem.* **1961**, *39*, 745.
4. Poling, G. W.; Leja, J. *J. Phys. Chem.* **1963**, *67*, 2121.
5. Colthup, N. B.; Daly, L. H.; Wiberley, S. E. *Introduction to Infrared and Raman Spectroscopy*, 3rd Ed.; Academic Press: San Diego; 1990; Chapt. 5.
6. Mielczarski, J. *Colloids and Surfaces* **1986**, *17*, 251.
7. Cases, J. M.; de Donate, P.; Kongolo, M.; Michot, L. *SME Annual Meeting*, 1989; preprint 89-62.
8. Leppinen, J. O. *Int. J. Miner. Process.* **1990**, *30*, 245.
9. Hodgson, M.; Agar, G. E. *Can. Met. Qtr.* **1989**, *28*, 189.
10. Hodgson, M.; Agar, G. E. *SME Annual Meeting* **1985**; preprint 85-24.
11. Hamilton, I. C.; Woods, R. *J. Electroanal. Chem.* **1981**, *118*, 327.
12. Rao, S. R.; Finch, J. A. *Can. Met. Qtr.* **1991**, *30*, 1.